https://doi.org/10.67571/njeru.2025.010818
NIGERIAN JOURNAL OF ENGINEERING RESEARCH UNICROSS (NJERU)
Volume 2, Issue 1, 1st May, 2025

Hydrogen blending vs waste-heat recovery in large dual-fuel engines: A prospective lifecycle techno-economic and probabilistic assessment

Samuel Oliver Effiom[a*]
[a] *Department of Mechanical Engineering, University of Cross River State, Calabar, Nigeria*

*Corresponding author Email: samueloliver@unicross.edu.ng

Received: 20th March, 2025 Reviewed: 22nd April, 2025 Accepted: 1st May, 2025

ABSTRACT
Hydrogen blending is increasingly proposed as a near-term route for decarbonising gas-fired power and propulsion systems, but volumetric blend percentages are often interpreted as equivalent energetic substitution. This study asks a practical design question: under what conditions does hydrogen blending provide greater climate and economic value than recovering exhaust heat from a large dual-fuel engine? A prospective cradle-to-busbar model was developed for an 18V50DF-class engine using an official simple-cycle efficiency of 49.4% and a waste-heat-recovery efficiency ceiling of 54.0%. Hydrogen fractions of 0-30 vol% were converted to energy shares using lower heating values, and lifecycle greenhouse-gas (GHG) intensity included combustion CO2, upstream natural-gas emissions, methane slip, hydrogen production emissions and the indirect warming effect of hydrogen leakage. Fuel cost, annualised waste-heat-recovery cost and carbon cost were evaluated alongside a 50,000-sample uncertainty analysis. Twenty vol% hydrogen supplied only 7.01% of fuel energy. In the central case, it lowered GHG intensity from 514.3 to 489.4 g CO2e kWh-1 (4.8%) but increased cost from 8.10 to 9.31 US cents kWh-1 at a US$50 tCO2e-1 carbon price. Waste-heat recovery alone reduced GHG intensity to 470.5 g CO2e kWh-1 (8.5%) and cost to 7.69 US cents kWh-1. The combined 20 vol% H2-WHR case reached 447.8 g CO2e kWh-1 (12.9%). The central break-even hydrogen price was US$1.19 kg-1, and hydrogen carbon intensity had to remain below 8.27 kg CO2e kgH2-1 for net climate benefit. Within the adopted uncertainty distributions, waste-heat recovery dominated the baseline on both metrics in 99.4% of samples, compared with 0.1% for hydrogen blending alone. The results support an efficiency-first hierarchy: recover avoidable heat before using scarce low-carbon hydrogen, unless hydrogen is demonstrably low-cost, low-emission and operationally compatible with the engine.

Keywords: Renewable dual-fuel engine; hydrogen blending; waste-heat recovery; methane slip; lifecycle assessment; techno-economic analysis; uncertainty; propulsion decarbonisation

I. INTRODUCTION

Rapid decarbonisation of electricity and transport must proceed while power systems retain enough flexibility to balance variable renewable generation. Reciprocating gas engines remain relevant in isolated grids, industrial cogeneration, peak-load generation and marine propulsion because they can start quickly, operate efficiently at modular scales and use established gaseous-fuel infrastructure. Their climate performance, however, depends on more than stack carbon dioxide. Upstream methane emissions and unburned methane released from the engine can materially erode the nominal carbon advantage of natural gas, particularly when engines operate away from their optimum load [1,10,11].

Hydrogen-natural-gas blends are frequently presented as a transitional fuel. Hydrogen contains no carbon at the point of combustion and can accelerate flame propagation, widen lean-burn limits and alter methane oxidation. These effects may improve combustion stability in some engines, although they can also increase abnormal-combustion risk, heat-transfer losses and nitrogen-oxide formation if calibration is not redesigned [7-9,23]. The word 'blend' can also be misleading. Pipeline and engine proposals are normally expressed on a volumetric or molar basis, whereas carbon displacement is governed primarily by energy fraction. Because hydrogen has a much lower volumetric heating value than methane-rich natural gas, 20 vol% hydrogen represents far less than 20% of the supplied chemical energy.

A second decarbonisation route is to reduce fuel demand rather than change fuel composition. Exhaust-gas and cooling-water heat from large engines can be recovered through steam or organic Rankine cycles, combined-cycle arrangements, thermoelectric devices or integrated heat-use systems. Previous studies have demonstrated technical and economic potential for engine waste-heat recovery, but the reported benefit is strongly case-specific because exhaust temperature, duty cycle, working fluid, heat-sink conditions and capital cost vary [18-22]. For a commercial 18V50DF-class engine, the published full-load electrical efficiency is 49.4%, while combined-cycle configurations can exceed 54% [24,25]. This difference creates a useful, real-world benchmark against which low-level hydrogen blending can be assessed.

Lifecycle climate accounting further complicates the comparison. Hydrogen production can range from very low emissions when electrolysis uses additional renewable electricity to high emissions when grid electricity or fossil pathways dominate [4-6]. Hydrogen leakage also has an indirect warming effect because it changes atmospheric methane, ozone and stratospheric water vapour. Recent multi-model work estimates a 100-year GWP of 11.6 +/- 2.8 kg CO_2e per kilogram of emitted hydrogen [12-17]. Consequently, a hydrogen blend is not automatically low-carbon; its benefit depends jointly on the displaced natural gas, hydrogen production pathway, hydrogen losses, methane slip and the time horizon used for climate assessment.

The literature contains detailed engine-combustion studies, hydrogen supply-chain assessments and waste-heat-recovery optimisation studies, but these streams are rarely combined into one decision framework for a commercially relevant large dual-fuel engine. In particular, few studies compare a volumetrically specified hydrogen blend against an efficiency retrofit while simultaneously accounting for methane slip, hydrogen leakage, lifecycle fuel emissions, carbon pricing and parameter uncertainty. This omission can lead operators to prioritise a visible fuel switch over a less visible efficiency measure even when the latter avoids more emissions at lower cost.

This paper therefore addresses the following research question: when does hydrogen blending outperform waste-heat recovery as a decarbonisation option for a large flexible dual-fuel engine? The study contributes (i) an explicit volume-to-energy correction for hydrogen-natural-gas blends; (ii) a unified cradle-to-busbar GHG and cost model; (iii) a multi-objective comparison of hydrogen fraction and waste-heat-recovery deployment; and (iv) a probabilistic assessment of climate and cost dominance. The intention is not to certify a particular retrofit. Rather, the model provides a transparent screening tool for power-plant and propulsion decisions before detailed combustion, safety, materials and OEM studies are undertaken.

II. LITERATURE CONTEXT AND RESEARCH GAP

A. Hydrogen-enriched Gaseous-fuel Combustion:

Hydrogen changes the thermophysical and kinetic behaviour of gaseous fuels. It has a high gravimetric LHV, low volumetric LHV, wide flammability range, low ignition energy and high laminar flame speed. Reviews by Taamallah et al. [23] and Algayyim et al. [7] show that these properties can improve flame stability and lean combustion, but they also narrow the margin to pre-ignition and flashback and may increase NOx where peak temperatures rise. The net efficiency response is therefore engine- and calibration-specific rather than an intrinsic property of the blend.

Experimental work on a heavy-duty spark-ignition engine found measurable changes in performance and emissions with hydrogen-natural-gas blends [8]. Numerical work for a marine dual-fuel engine similarly indicated that hydrogen addition can reduce methane slip by improving oxidation, although the magnitude depends on mixture preparation and engine geometry [9]. These studies justify an optional methane-slip reduction in sensitivity analysis, but they do not support transferring a fixed efficiency or slip benefit directly to an 18V50DF-class engine. The central model therefore assumes no hydrogen-induced efficiency improvement and no additional methane-slip benefit beyond the lower methane throughput. This conservative choice prevents a literature effect from being treated as an engine-specific measurement.

B. Methane Slip and Lifecycle Climate Performance:

Methane slip is a defining uncertainty for lean-burn and dual-fuel gas engines. It arises from crevice volumes, quenching near cold surfaces, incomplete oxidation and scavenging or valve-overlap processes. Huonder and Olsen [10] review in-cylinder and after-treatment options, while ship measurements by Balcombe et al. [11] demonstrate that real-world methane emissions vary with engine technology and operating condition. For this reason, the analysis represents baseline slip as a probability distribution rather than a single universal emission factor.

The climate effect of hydrogen leakage has moved from a peripheral issue to a central boundary condition in hydrogen lifecycle analysis. Ocko and Hamburg [12] demonstrated the short-term warming consequences of emitted hydrogen; Hauglustaine et al. [13] and Bertagni et al. [14] showed that production route and leakage jointly govern system benefit. Sand et al. [15] provided a multi-model GWP100 estimate, while Sun et al. [16] and Goita et al. [17] integrated hydrogen and methane emissions into use-case and supply-chain assessments. Collectively, these studies support treating hydrogen CI and leakage as independent variables rather than assigning a single label such as 'green' or 'blue'.

C. Engine waste-heat recovery

Waste-heat recovery converts a fraction of otherwise rejected heat into useful power or heat. Valencia Ochoa et al. [18] combined exergy, economic and lifecycle assessment for an ORC coupled to a natural-gas engine. Larsen et al. [19] and Liu et al. [20] explored cycle configuration and optimisation for marine engines, while Diaz-Secades et al. [21] used preference learning and Bayesian optimisation for a hybrid marine WHR system. Wang et al. [22] further demonstrated multi-objective optimisation of a natural-gas-engine/ORC system. These studies consistently show that WHR performance is sensitive to heat-source conditions and economic assumptions; they also establish that efficiency improvements should be evaluated alongside emissions rather than as a purely thermodynamic exercise.

The unresolved comparison is strategic rather than component-specific. Hydrogen blending reduces the carbon content of a fraction of the fuel but introduces an expensive energy carrier and a new lifecycle boundary. WHR leaves the fuel unchanged but reduces the amount required for every delivered kilowatt-hour. A consistent functional unit and common uncertainty space are therefore required to determine which option should be implemented first.

III. MATERIAL AND METHODS

A. Study design, case engine and functional unit

A prospective attributional screening model was constructed in Python. The functional unit was 1 kWh of net electricity delivered at the generator busbar. The model boundary included natural-gas supply, hydrogen supply, fuel blending, engine conversion, methane slip, direct combustion CO2 and WHR capital and operation. Common engine fixed operation and maintenance costs were excluded because they do not change the ranking of the alternatives. Hydrogen storage, compression, delivery infrastructure and engine-conversion capital were also excluded from the central cost comparison because site-specific data were unavailable; this makes the hydrogen result deliberately favourable and is discussed as a limitation.

The reference unit was an 18-cylinder 50DF-class engine rated at 17.635 MW with an official electrical efficiency of 49.4% and heat rate of approximately 7,285 kJ kWh-1 [24]. The heat-rate consistency check gives 3,600/7,285 = 49.42%, which agrees with the stated efficiency. A full WHR configuration was represented by a net electrical efficiency of 54.0%, consistent with the manufacturer's published combined-cycle performance [25]. Intermediate WHR deployment was interpolated linearly for the multi-objective design space.

B. Hydrogen volume-to-energy conversion

For ideal gas mixtures at common temperature and pressure, volume fraction equals mole fraction. The hydrogen energy fraction was calculated from the component volumetric LHVs rather than equating energy share with blend volume:

$$y\_H2 = (x\_H2\ LHV\_H2,vol) / [x\_H2\ LHV\_H2,vol + (1 - x\_H2)\ LHV\_NG,vol] \quad (1)$$

where xH2 is the hydrogen volume fraction, yH2 is the hydrogen energy fraction, LHVH2,vol = 10.8 MJ Nm-3 and LHVNG,vol = 35.8 MJ Nm-3. The selected values represent hydrogen and methane-rich natural gas on an LHV basis. Component mass flows followed from LHVs of 120 MJ kg-1 for hydrogen and 50 MJ kg-1 for methane. Fig. 1. Depicts the relationship between hydrogen volume fraction and energetic substitution. The dashed line shows the commonly implied but incorrect one-to-one assumption.

C. Efficiency and energy-flow model

Net efficiency was represented as a continuous decision variable between the simple-cycle and combined-cycle values:

$$eta\_net = eta\_engine + f\_WHR\ (eta\_CC - eta\_engine) \quad (2)$$

where fWHR ranges from 0 to 1, etaengine = 0.494 and etaCC = 0.540. The required fuel heat input was:

$$Q\_fuel = 3.6 / eta\_net \quad (3)$$

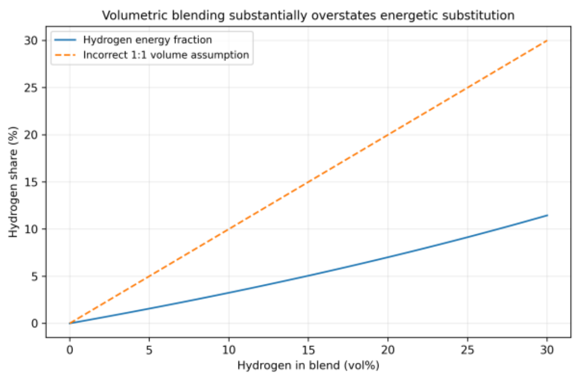

Figure. 1. Relationship between hydrogen volume fraction and energetic substitution.

with Qfuel in MJ per net kWh. Hydrogen and methane energy inputs were yH2 Qfuel and (1-yH2) Qfuel, respectively. The central analysis held engine efficiency constant with hydrogen fraction because no validated performance map was available for the reference engine on the prospective blends. A +/- sensitivity around the WHR efficiency ceiling was included in the uncertainty analysis.

B. Lifecycle greenhouse-gas model

For Lifecycle GHG intensity was calculated as the sum of five terms:

$$GHG = CO2\_comb + GHG\_NG,up + GHG\_CH4,slip + GHG\_H2,prod + GHG\_H2,leak \quad (4)$$

Combustion CO_2 was based on 2.75 kg CO_2 per kilogram of methane burned. Natural-gas upstream emissions were applied to methane energy input. Baseline methane slip was specified in grams of CH_4 per net kWh and scaled with methane energy throughput; the central value was 1.5 g kWh^{-1} and the uncertainty range was 0.5-5.0 g kWh^{-1}. This range is intended to span well-controlled high-load operation and less favourable operation reported in the engine and shipping literature [10,11]. Slipped methane was assigned GWP100 = 29.8 kg CO_2e $kgCH_4^{-1}$, consistent with AR6 central values for fossil methane [26].

Hydrogen production emissions were the delivered hydrogen mass multiplied by its lifecycle CI. Leakage was represented as the fraction lost before useful combustion, and the leaked mass was assigned GWP100 = 11.6 kg CO_2e kgH_2^{-1}, with uncertainty of +/-2.8 based on the multi-model assessment by Sand et al. [15]. The principal analysis used GWP100 to align with common lifecycle and policy practice. The model does not imply that GWP100 captures every short-term climate concern; Ocko and Hamburg [12] and Sun et al. [16] show that shorter horizons can make leakage more consequential.

C. Cost model

Net The cost metric comprised fuel, annualised WHR capital and fixed WHR maintenance, plus an optional carbon cost. Natural gas was priced per MMBtu and hydrogen per delivered kilogram. The WHR annualisation used a capital recovery factor:

$$CRF = i(1 + i)^n / [(1 + i)^n - 1] \quad (5)$$

where i is the real discount rate and n is project life. Recovered power was calculated from the efficiency ratio at constant engine fuel input. WHR CAPEX was applied per kilowatt of recovered power, then divided by annual net generation. The central assumptions were US$1,800 $kWrec^{-1}$, 8% WACC, 20-year life, fixed O&M equal to 2.5% of CAPEX per year and 80% capacity factor. These are screening assumptions rather than a vendor quotation. The uncertainty range of US$1,000-3,000 $kWrec^{-1}$ reflects the site-specific nature of small and medium WHR systems reported in the literature [18-22].

A carbon price was applied to total lifecycle GHG rather than stack CO_2 alone. Marginal abatement cost excluded the carbon payment to avoid counting the policy instrument as a physical resource cost:

$$MAC = (C\_scenario,no\text{-}carbon - C\_baseline,no\text{-}carbon) / (GHG\_baseline - GHG\_scenario) \quad (6)$$

The central assumptions and uncertainty distributions are presented in Table 1.

D. Scenario, multi-objective and uncertainty analyses

Seven central scenarios were evaluated: the natural-gas baseline; 10, 20 and 30 vol% hydrogen without WHR; WHR without hydrogen; and 20 and 30 vol% hydrogen with full WHR. A design grid combined 31 hydrogen fractions with 21 WHR deployment levels. A point was considered non-dominated when no other point had both lower GHG intensity and lower cost.

Parameter uncertainty was propagated through 50,000 independent triangular or truncated-normal samples. Common random draws were used across scenarios so that scenario differences were paired. Results are reported as medians and 5th-95th percentile intervals. Spearman rank correlations identified the parameters most strongly associated with incremental GHG and cost. Two analytical thresholds were also calculated: the hydrogen price that makes 20 vol% blending cost-neutral relative to the baseline, and the maximum hydrogen CI that preserves a lifecycle GHG benefit.

E. Model verification and reproducibility

Three checks were applied. First, the efficiency calculated from the published heat rate reproduced the manufacturer value to two decimal places. Second, the zero-hydrogen, zero-WHR case reduced algebraically to the methane-only balance.

TABLE 1.
CENTRAL ASSUMPTIONS AND DISTRIBUTIONS USED IN THE 50,000-SAMPLE UNCERTAINTY ANALYSIS.

Parameter	**Central value**	**Uncertainty distribution**	**Basis**
Engine efficiency	49.4%	Fixed	Manufacturer data [24]
Full WHR efficiency	54.0%	Triangular 53-54-55%	Manufacturer benchmark [25]
NG upstream intensity	10 kg CO2e GJ-1	Triangular 4-10-20	Lifecycle screening; [11,17]
H2 lifecycle CI	2.5 kg CO2e kg-1	Triangular 0.5-2.5-8.0	Prospective low-carbon range; [4-6,17]
H2 leakage	1.0%	Triangular 0.1-1.0-5.0%	Supply-chain uncertainty; [12-17]
H2 GWP100	11.6	Normal 11.6 +/- 2.8, truncated	Multi-model estimate [15]
CH4 GWP100	29.8	Normal 29.8 +/- 4.0, truncated	IPCC AR6 [26]
Baseline CH4 slip	1.5 g kWh-1	Triangular 0.5-1.5-5.0	Engine literature [10,11]
Natural-gas price	US$8 MMBtu-1	Triangular 4-8-14	Scenario variable
Hydrogen price	US$4 kg-1	Triangular 2-4-8	Hydrogen literature [4-6,27,28]
Carbon price	US$50 tCO2e-1	Triangular 0-50-200	Policy scenario
WHR CAPEX	US$1,800 kWrec-1	Triangular 1,000-1,800-3,000	Screening range [18-22]
WACC	8%	Triangular 5-8-12%	Financing scenario
Project life	20 y	Triangular 15-20-25 y	Engineering assumption
Capacity factor	80%	Triangular 50-80-92%	Dispatch scenario

Third, all scenario results were recomputed from a saved input table and compared with the generated central-results file. The analysis script, central results, design grid, sensitivity table and compressed 50,000-sample dataset accompany the manuscript as supplementary files.

This is a prospective model, not an engine test. Hydrogen fractions above the currently approved specification of any specific installation require OEM agreement, hazard assessment, control-system review and verification of fuel-system materials. The model therefore estimates system-level potential and should not be interpreted as operational authorisation.

IV. RESULTS

A. Volumetric blend fraction versus energy substitution

The nonlinear conversion in Eq. (1) is the first-order result. Hydrogen fractions of 10, 20 and 30 vol% corresponded to only 3.24, 7.01 and 11.45% of fuel energy, respectively. At unchanged efficiency, these values also set the approximate upper limit on direct fossil-carbon displacement before lifecycle effects are included. Thus, interpreting a 20 vol% blend as a 20% decarbonisation measure overstates energetic substitution by almost a factor of three. The Central lifecycle and cost results is presented in Table 2.

The baseline lifecycle intensity was 514.3 g CO2e kWh-1. Hydrogen blending reduced this value monotonically, but the improvement was modest relative to the stated volumetric fraction. The 20 vol% case reached 489.4 g CO2e kWh-1, a 4.83% reduction, while 30 vol% reached 473.8 g CO2e kWh-1, a 7.88% reduction. At US$4 kg-1 hydrogen, however, the 20 vol% blend increased the carbon-inclusive cost by 1.21 US cents kWh-1 and had a marginal abatement cost of approximately US$537 tCO2e-1.

WHR alone produced a larger GHG reduction than 20 or 30 vol% hydrogen because the efficiency increase reduced every fuel-related term per delivered kilowatt-hour. GHG intensity fell by 8.52% to 470.5 g CO2e kWh-1. Fuel savings more than offset annualised WHR cost in the central case, lowering the carbon-inclusive cost from 8.10 to 7.69 US cents kWh-1. The negative marginal abatement cost (-US$44 tCO2e-1) indicates that the efficiency measure saved money before carbon pricing.

The combined configurations provided the deepest reductions. Twenty vol% hydrogen plus WHR reached 447.8 g CO2e kWh-1, 12.93% below baseline; 30 vol% plus WHR reached 433.4 g CO2e kWh-1, 15.72% below baseline. The combined 20 vol% case still cost 0.69 US cents kWh-1 more than baseline at central assumptions, showing that technical complementarity does not automatically imply economic parity. Fig. 2. Depicts the central-case lifecycle GHG intensity and cost trade-off for the seven scenarios.

TABLE II.

CENTRAL SCENARIO RESULTS. COST INCLUDES FUEL, WHR COST AND A US$50 TCO2E-1 LIFECYCLE CARBON PRICE; MAC EXCLUDES THE CARBON PAYMENT.

Scenario	H2 energy (%)	Efficiency (%)	GHG (g CO2e/kWh)	Reduction (%)	Cost (US cents/kWh)	MAC (US$/tCO2e)
Baseline NG engine	0.00	49.4	514.3	0.00	8.10	-
H2-10 (10 vol%)	3.24	49.4	502.8	2.23	8.66	537.4
H2-20 (20 vol%)	7.01	49.4	489.4	4.82	9.31	537.4
H2-30 (30 vol%)	11.45	49.4	473.8	7.88	10.07	537.4
WHR only	0.00	54.0	470.5	8.52	7.68	-44.1
H2-20 + WHR	7.01	54.0	447.8	12.93	8.79	154.4
H2-30 + WHR	11.45	54.0	433.4	15.72	9.49	222.4

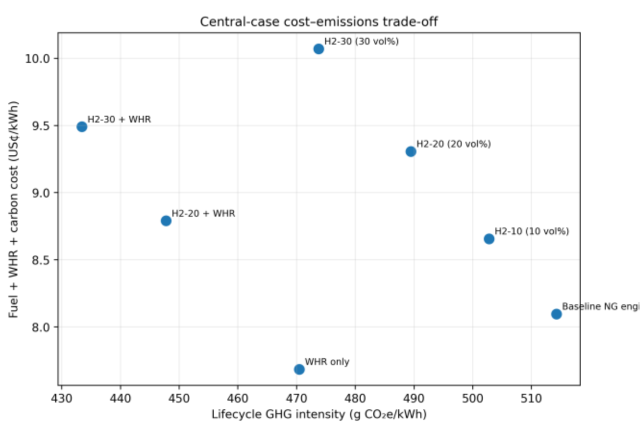

Figure. 2. Central-case lifecycle GHG intensity and cost trade-off for the seven scenarios.

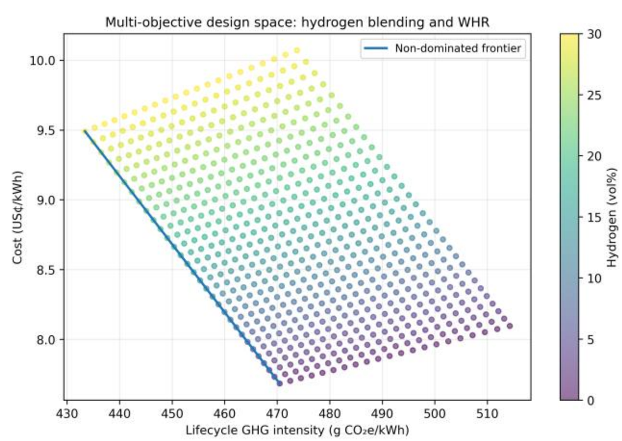

Figure. 3. Central multi-objective design space.

TABLE III

. MONTE CARLO UNCERTAINTY RESULTS FROM 50,000 COMMON-RANDOM-NUMBER SAMPLES.

Scenario	GHG median (5-95%), g CO2e/kWh	Cost median (5-95%), US cents/kWh
Baseline	544.3 (490.8-611.5)	10.33 (6.39-15.43)

Scenario	GHG median (5-95%), g CO2e/kWh	Cost median (5-95%), US cents/kWh
H2-20	517.7 (468.0-577.2)	11.73 (7.90-16.61)
WHR	498.1 (448.4-560.0)	9.79 (6.18-14.46)
H2-20+WHR	473.6 (427.8-528.6)	11.08 (7.56-15.55)

B. Volumetric blend fraction versus energy substitution

For the 20 vol% case, the central delivered hydrogen price required for cost parity with the natural-gas baseline was US$1.19 kg-1. This threshold already credits a US$50 tCO2e-1 carbon price and excludes hydrogen storage, compression, blending-station and engine-modification capital. It is therefore an optimistic plant-gate threshold. At a delivered hydrogen price of US$4 kg-1, carbon pricing alone would need to rise substantially, or natural-gas price would need to increase, before the blend became cost-neutral.

The maximum lifecycle hydrogen CI that preserved a GHG benefit for 20 vol% blending was 8.27 kg CO2e kgH2-1 in the central case. This threshold is not a universal sustainability label; it changes with methane slip, upstream natural-gas intensity, leakage and the displaced-fuel benchmark. It does, however, show that high-emission hydrogen can eliminate the already modest benefit associated with low-energy-share blending.

C. Multi-objective design space

The design grid produced a curved cost-emissions envelope rather than a single optimum. Increasing WHR deployment moved solutions down and left because it reduced both fuel use and carbon cost, while increasing hydrogen fraction generally moved solutions left and up because emissions declined but fuel cost rose. The non-dominated frontier therefore applied WHR before substantial hydrogen blending under central conditions. Low-WHR, high-hydrogen combinations were dominated by configurations that achieved comparable GHG intensity with greater heat recovery and less hydrogen. Fig. 3. depicts the central multi-objective design space. Colour indicates hydrogen volume fraction; the solid line is the non-dominated cost-emissions frontier. The uncertainty propagation is tabulated in Table 3.

The uncertainty bands overlapped, but the ranking of median GHG intensity remained stable: combined H2-WHR was lowest, followed by WHR, H2-20 and the baseline. Median baseline GHG intensity was 544.3 g CO2e kWh-1 because triangular sampling places substantial probability above the central methane-slip and upstream-emission assumptions. Median values were 517.7 g CO2e kWh-1 for H2-20, 498.1 for WHR and 473.6 for the combined case.

Within the adopted distributions, all three interventions had lower lifecycle GHG intensity than the paired baseline in essentially all samples. Cost dominance differed sharply. H2-20 cost less than baseline in only 0.1% of samples. WHR cost less in 99.4%, and the combined system cost less in 13.1%. These probabilities are conditional on the stated distributions, especially the exclusion of hydrogen retrofit capital and the assumed WHR cost range; they should not be interpreted as universal frequencies. Fig. 5. Depicts the lifecycle GHG medians and 5th-95th percentile intervals from the uncertainty analysis.

D. Sensitivity drivers -

Fig. 6. depicts the Spearman rank correlations for incremental GHG and cost of the 20 vol% hydrogen case. Hydrogen lifecycle CI was the dominant driver of the incremental GHG result for H2-20, followed by baseline methane slip, the assumed additional slip reduction, upstream natural-gas intensity and methane GWP. Hydrogen price overwhelmingly controlled incremental cost. Carbon price and natural-gas price partially offset the hydrogen premium because the blend avoided some lifecycle emissions and methane-rich fuel. Hydrogen leakage had a smaller GWP100 influence than production CI within the adopted range, consistent with Goita et al. [17], but its importance would increase under a shorter time horizon or a higher-leakage supply chain [12,15,16].

V. DISCUSSION

A. Why efficiency-first outperforms low-volume hydrogen blending

The The comparison is governed by two asymmetries. First, hydrogen occupies a large fraction of gas volume but a small fraction of fuel energy. At 20 vol%, only 7.01% of energy is carbon-free at the engine boundary. Second, WHR reduces all fuel-related flows per net kilowatt-hour: combusted methane, upstream gas emissions, methane slip and any hydrogen that might later be blended. A 49.4-to-54.0% efficiency increase reduces heat input by 8.52%, which is larger than the energetic substitution provided by 20 vol% hydrogen. This explains why WHR achieved the larger standalone reduction without relying on low-carbon fuel availability.

The result does not imply that hydrogen has no role in engine decarbonisation. It shows that low-volume blending is a relatively weak use of scarce low-carbon hydrogen when unrecovered exhaust energy remains available. Hydrogen becomes more attractive when (i) WHR potential has already been exploited; (ii) delivered hydrogen price approaches the avoided natural-gas and carbon cost; (iii) hydrogen CI is demonstrably below the displacement threshold; (iv) leakage is controlled; and (v) combustion calibration can capture efficiency or methane-slip benefits without unacceptable NOx or durability penalties [28-30].

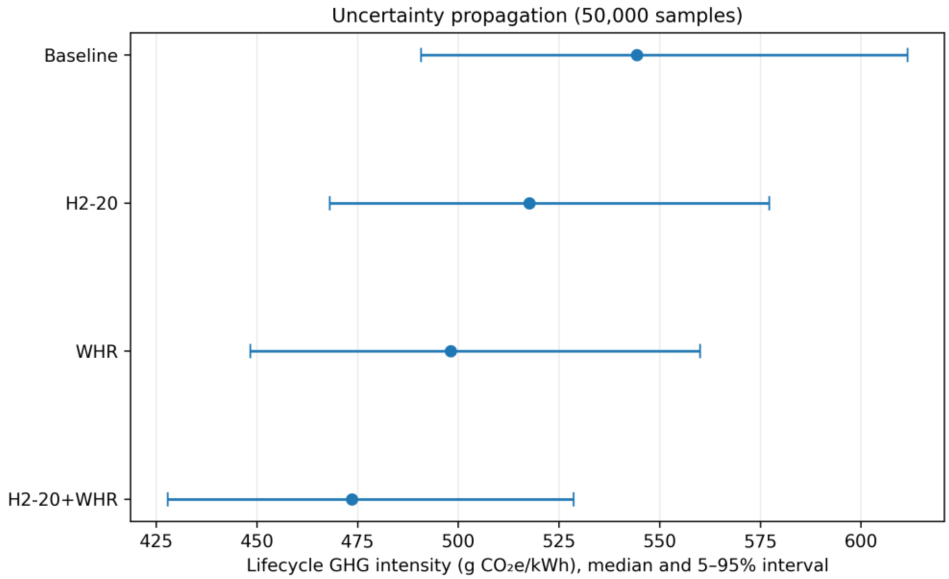

Fig. 5. Lifecycle GHG medians and 5th-95th percentile intervals from the uncertainty analysis.

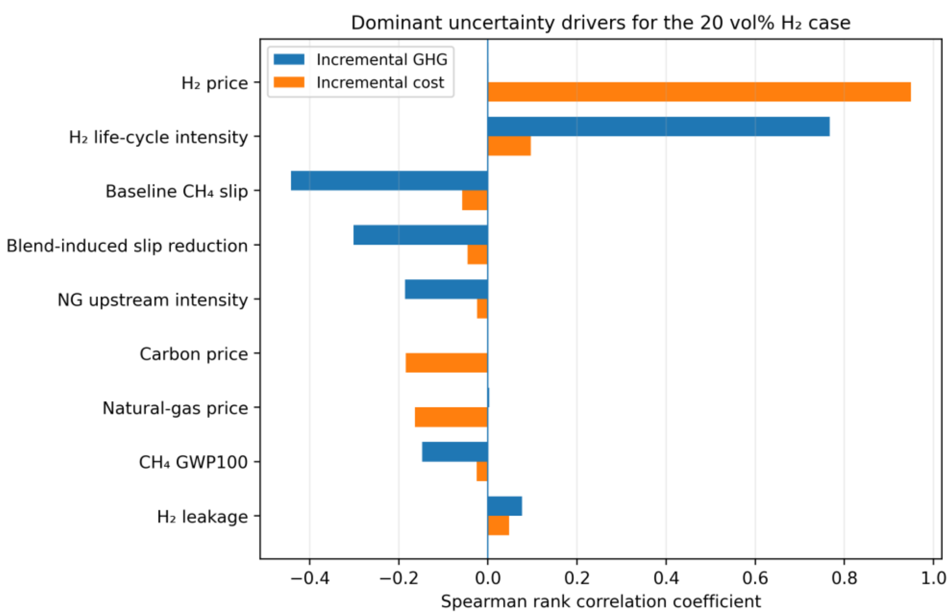

Fig. 6. Spearman rank correlations for incremental GHG and cost of the 20 vol% hydrogen case.

B. Implications for sustainable power and propulsion systems

For flexible power plants, the operational order matters. WHR performs best at sustained medium-to-high load, while peaking plants may not supply enough stable exhaust heat to justify a bottoming cycle. Conversely, the economic value of fast-start flexibility can favour simple-cycle operation. The capacity-factor distribution in this study captures part of this tension, but a plant-specific dispatch model should precede investment. Where thermal demand exists, combined heat and power may outperform electricity-only WHR and should be included in future extensions.

For marine propulsion, the same hierarchy is relevant but the boundary must include vessel load profiles, space and mass constraints, fuel-tank volume, class rules and voyage-specific carbon regulation. Hydrogen's low volumetric energy density is especially consequential onboard, while WHR equipment adds mass and complexity. The present engine-class analysis is therefore transferable as a screening framework, not as a ship design. A propulsion study should couple the model to measured engine maps, weather-routing loads and fuel-storage penalties.

For African power systems, local hydrogen cost and financing are decisive. Egli et al. [5] found that African green-hydrogen exports remain sensitive to financing and policy support, with least-cost 2030 estimates still above the central break-even threshold found here. Locally produced hydrogen may avoid conversion and shipping costs, but electrolysis electricity, water treatment, compression and capacity utilisation remain material. This reinforces the value of first reducing avoidable fuel consumption in existing assets.

C. Methane and hydrogen leakage as decision variables

A notable result is that baseline methane slip increases the apparent climate value of hydrogen because blending displaces methane throughput and may improve oxidation. This does not justify tolerating methane slip. It means that engine-specific methane measurement is essential before assigning credit to a fuel change. Direct methane-control measures, including calibration, crevice-volume reduction, oxidation catalysts and load management, may deliver cheaper abatement than either hydrogen blending or WHR in high-slip installations [10].

Hydrogen leakage was less influential than production CI on a GWP100 basis in the adopted range, but it should not be dismissed. Leakage is a preventable loss of an expensive fuel, creates safety concerns and has a stronger near-term climate effect than its 100-year metric suggests [12,15,16]. Procurement contracts should therefore specify both lifecycle CI and measured supply-chain loss rather than relying solely on a production colour label.

D. Comparison with prior studies

The combustion literature generally reports lower carbon-containing exhaust species and faster combustion with hydrogen addition, alongside context-dependent efficiency and NOx responses [7-9,23,30]. The present study does not contradict these findings; it isolates the system-level consequence of the blend's energy content and lifecycle supply. Even when hydrogen improves methane oxidation, the amount of fossil energy displaced by a 20 vol% blend remains approximately 7%.

The WHR result is consistent with studies that report meaningful fuel savings from Rankine-cycle and hybrid recovery systems [18-22,29]. The exact 8.52% reduction here is not a universal ORC performance claim; it follows from the manufacturer-based efficiency comparison used for the case engine. The contribution is the common comparison boundary: the same engine output, lifecycle emissions and cost accounting are applied to both fuel substitution and efficiency improvement.

E. Limitations and research needs

i. The engine model is steady-state and uses a manufacturer full-load efficiency rather than a measured part-load map. Real dispatch can change efficiency, methane slip and exhaust-heat quality simultaneously.
ii. Hydrogen-induced changes in efficiency, NOx, knock margin, turbocharger operation and component temperatures are not modelled. These require engine-specific experiments or validated one-/three-dimensional simulations.
iii. Hydrogen infrastructure and engine-conversion capital are excluded, making the hydrogen cost comparison optimistic. WHR integration costs are represented by a screening range rather than a site quotation.
iv. Natural gas is represented as methane-rich fuel with fixed heating values. Actual gas composition, pilot-fuel consumption and pilot-fuel emissions should be added for a detailed 50DF assessment.
v. Only GWP100 is reported in the principal results. A future paper should present GWP20 and dynamic temperature-response metrics to reflect near-term methane and hydrogen forcing.
vi. The study evaluates electricity-only WHR. Useful heat, cooling, desalination or process integration could materially improve project economics.
vii. The uncertainty analysis represents epistemic ranges but does not replace validation data. A publishable follow-on experimental paper should measure fuel composition, mass flow, electrical output, exhaust temperature, CH4, CO2, NOx and O2 across load and blend fraction.

VI. Conclusion

i. The Blend percentages must be converted from volume to energy before decarbonisation claims are made. Ten, 20 and 30 vol% hydrogen supplied only 3.24, 7.01 and 11.45% of fuel energy.
ii. At central assumptions, 20 vol% hydrogen lowered lifecycle GHG intensity by 4.83% but increased cost by 1.21 US cents kWh-1. Its marginal abatement cost was approximately US$537 tCO2e-1 before counting hydrogen retrofit infrastructure.
iii. Raising net efficiency from 49.4 to 54.0% through WHR reduced lifecycle GHG intensity by 8.52% and lowered cost in the central case. It dominated the baseline in 99.4% of uncertainty samples.
iv. Combining 20 vol% hydrogen with WHR produced a 12.93% central GHG reduction, demonstrating technical complementarity, but it remained more expensive than baseline at a US$4 kg-1 hydrogen price.
v. The central break-even hydrogen price was US$1.19 kg-1, and hydrogen CI had to remain below 8.27 kg CO2e kgH2-1 to preserve net benefit. These thresholds are conditional on methane slip, gas supply emissions, leakage and carbon price.
vi. The practical hierarchy is therefore efficiency first, methane control second and low-carbon hydrogen where its cost, lifecycle intensity, leakage and engine compatibility are verified.

References

[1] IPCC. Climate Change 2023: Synthesis Report. Contribution of Working Groups I, II and III to the Sixth Assessment Report of the Intergovernmental Panel on Climate Change. Geneva: IPCC; 2023. https://doi.org/10.59327/IPCC/AR6-9789291691647.001.

[2] International Energy Agency. Global Hydrogen Review 2024. Paris: IEA; 2024.

[3] Ueckerdt F, Bauer C, Dirnaichner A, Everall J, Sacchi R, Luderer G. Potential and risks of hydrogen-based e-fuels in climate change mitigation. Nature Climate Change 2021;11:384-393. https://doi.org/10.1038/s41558-021-01032-7.

[4] Ueckerdt F, Verpoort PC, Anantharaman R, Bauer C, Beck F, Longden T, Roussanaly S. On the cost competitiveness of blue and green hydrogen. Joule 2024;8:104-128. https://doi.org/10.1016/j.joule.2023.12.004.

[5] Egli F, Schneider F, Leonard A, Halloran C, Salmon N, Schmidt T, Hirmer S. Mapping the cost competitiveness of African green hydrogen imports to Europe. Nature Energy 2025;10:750-761. https://doi.org/10.1038/s41560-025-01768-y.

[6] Koj JC, Zapp P, Wieland C, Görner K, Kuckshinrichs W. Life cycle environmental impacts and costs of water electrolysis technologies for green hydrogen production in the future. Energy, Sustainability and Society 2024;14:64. https://doi.org/10.1186/s13705-024-00497-6.

[7] Algayyim SJM, Saleh K, Wandel AP, Fattah IMR, Yusaf T, Alrazen HA. Influence of natural gas and hydrogen properties on internal combustion engine performance, combustion, and emissions: A review. Fuel 2024;362:130844. https://doi.org/10.1016/j.fuel.2023.130844.

[8] De Simio L, Iannaccone S, Guido C, Napolitano P, Maiello A. Natural Gas/Hydrogen blends for heavy-duty spark ignition engines: Performance and emissions analysis. International Journal of Hydrogen Energy 2024;50:743-757. https://doi.org/10.1016/j.ijhydene.2023.06.194.

[9] Xin M, Gan H, Cong Y, Wang H. Numerical simulation of methane slip from marine dual-fuel engine based on hydrogen-blended natural gas strategy. Fuel 2024;358:130132. https://doi.org/10.1016/j.fuel.2023.130132.

[10] Huonder A, Olsen D. Methane Emission Reduction Technologies for Natural Gas Engines: A Review. Energies 2023;16:7054. https://doi.org/10.3390/en16207054.

[11] Balcombe P, Heggo DA, Harrison M. Total Methane and CO2 Emissions from Liquefied Natural Gas Carrier Ships: The First Primary Measurements. Environmental Science & Technology 2022;56(13):9632-9640. https://doi.org/10.1021/acs.est.2c01383.

[12] Ocko IB, Hamburg SP. Climate consequences of hydrogen emissions. Atmospheric Chemistry and Physics 2022;22:9349-9368. https://doi.org/10.5194/acp-22-9349-2022.

[13] Hauglustaine DA, Paulot F, Collins WJ, Derwent RG, Sand M, Boucher O. Climate benefit of a future hydrogen economy. Communications Earth & Environment 2022;3:295. https://doi.org/10.1038/s43247-022-00626-z.

[14] Bertagni MB, Pacala SW, Paulot F, Porporato A. Risk of the hydrogen economy for atmospheric methane.

Nature Communications 2022;13:7706. https://doi.org/10.1038/s41467-022-35419-7.

[15] Sand M, Skeie RB, Sandstad M, Krishnan S, Myhre G, Bryant H, Derwent R, Hauglustaine D, Paulot F, Prather M, Stevenson D. A multi-model assessment of the Global Warming Potential of hydrogen. Communications Earth & Environment 2023;4:203. https://doi.org/10.1038/s43247-023-00857-8.

[16] Sun T, Shrestha E, Hamburg SP, Kupers R, Ocko IB. Climate Impacts of Hydrogen and Methane Emissions Can Considerably Reduce the Climate Benefits across Key Hydrogen Use Cases and Time Scales. Environmental Science & Technology 2024;58:5299-5309. https://doi.org/10.1021/acs.est.3c09030.

[17] Goita EG, Beagle EA, Nasta AN, Wissmiller DL, Ravikumar AP, Webber ME. Effect of hydrogen leakage on the life cycle climate impacts of hydrogen supply chains. Communications Earth & Environment 2025;6:160. https://doi.org/10.1038/s43247-025-02141-3.

[18] Valencia Ochoa G, Cárdenas Gutierrez JA, Duarte Forero J. Exergy, Economic, and Life-Cycle Assessment of ORC System for Waste Heat Recovery in a Natural Gas Internal Combustion Engine. Resources 2020;9:2. https://doi.org/10.3390/resources9010002.

[19] Larsen U, Pierobon L, Haglind F, Gabrielii C. Design and optimisation of organic Rankine cycles for waste heat recovery in marine applications using the principles of natural selection. Energy 2013;55:803-812. https://doi.org/10.1016/j.energy.2013.03.021.

[20] Liu X, Nguyen MQ, Chu J, Lan T, He M. A novel waste heat recovery system combining steam Rankine cycle and organic Rankine cycle for marine engine. Journal of Cleaner Production 2020;265:121502. https://doi.org/10.1016/j.jclepro.2020.121502.

[21] Díaz-Secades LA, González R, Rivera N, Montañés E, Quevedo JR. Waste heat recovery system for marine engines optimized through a preference learning rank function embedded into a Bayesian optimizer. Ocean Engineering 2023;281:114747. https://doi.org/10.1016/j.oceaneng.2023.114747.

[22] Wang C, Wang X, Wang H, Xu Y, Ge Y, Tan J, et al. Co-optimizing NOx emission and power output of a natural gas engine-ORC combined system through neural networks and genetic algorithms. Energy 2024;289:130072. https://doi.org/10.1016/j.energy.2023.130072.

[23] Taamallah S, Vogiatzaki K, Alzahrani FM, Mokheimer EMA, Habib MA, Ghoniem AF. Fuel flexibility, stability and emissions in premixed hydrogen-rich gas turbine combustion: Technology, fundamentals, and numerical simulations. Applied Energy 2015;154:1020-1047. https://doi.org/10.1016/j.apenergy.2015.04.044 .

[24] Wärtsilä. Wärtsilä 50DF dual-fuel engine for power plants: product data and performance. https://www.wartsila.com/energy/engine-power-plant-solutions/engine-power-plant-products/wartsila-50df-dual-fuel-engine. Accessed 18 May 2025.

[25] Wärtsilä. Flexicycle power plants: combined-cycle efficiency information. https://www.wartsila.com/energy/engine-power-plant-solutions/engine-power-plant-products/applications/flexicycle-power-plants. Accessed 24 June 2025.

[26] IPCC. Climate Change 2021: The Physical Science Basis. Cambridge: Cambridge University Press; 2021. https://doi.org/10.1017/9781009157896.

[27] International Renewable Energy Agency. Green Hydrogen Cost Reduction: Scaling up Electrolysers to Meet the 1.5 C Climate Goal. Abu Dhabi: IRENA; 2020.

[28] Udu, D. B., Effiom, S. O., Ovat, F. A., Abam, F. I., and Lawrence, E. (2025). Chemical looping reforming processes and recent advancements in oxygen carrier materials. Nile Journal of Engineering and Applied Science, 3(1), 135-148. https://doi.org/10.5455/NJEAS.217293

[29] Effiom, S. O., Udu, D. B., Abam, F. I., Effiom, P.-C. O., Bright, P., Onochie, O. C., Inah, O. I., Saeed, B., and Magu, T. O. (2025). Autothermal reforming process simulation and optimization of a biogas-based chemical looping for hydrogen production with CO_2 capture. Next Research, 3, Article 101109. https://doi.org/10.1016/j.nexres.2025.101109

[30] Frank, E., and Effiom, S. O. (2023). Development of a multigeneration system with integrated hydrogen production: A typical analysis. Nigerian Journal of Technology, 42(3), 330–338. https://doi.org/10.4314/njt.v42i3.5